

# Quantitative analysis of four EMG amplifiers

E.J. Perreault, I.W. Hunter and R.E. Kearney

Biomedical Engineering Department, McGill University, Montreal, Québec, Canada H3A 2B4

Received July 1991, accepted December 1992

## ABSTRACT

*Four typical EMG amplifiers were tested quantitatively to observe the diversity and specificity of available equipment. Gain, phase, common mode rejection ratio (CMRR) and noise characteristics were measured for each device. Various gain and phase responses were observed, each best suited to specific application areas. For all amplifiers, the CMRR was shown to decrease dramatically in the presence of input impedance mismatches of more than 10 k $\Omega$  between the two electrodes. Because such impedance mismatches are common on the skin surface, these results indicate that proper skin preparation is required to maximize the noise rejection capabilities of the tested amplifiers.*

**Keywords:** Electromyography, EMG signal processing, amplifier, frequency response, common mode rejection ratio, noise measurements

## INTRODUCTION

In 1849, 58 years after the monumental work of Galvani, DuBois-Reymond discovered a method for using skin surface recordings to measure the electrical activity elicited by voluntary muscular contractions<sup>1</sup>. Since that time, surface measurements of muscular electrical activity, electromyograms (EMGs), have become widely used clinical and research tools. Some of the most common uses for the EMG include: biofeedback, prosthetic control, and studies of reflexes and posture. Many of these applications use the EMG only to provide information on the level of muscular activity, based on the fact that the average measured EMG scales linearly with force during static, isometric conditions<sup>2-4</sup>. Other more quantitative uses for the electromyogram, such as spectral analysis and system identification, require accurate gain and phase recordings to provide meaningful results. Such techniques have proved useful in a variety of areas, including: analysing muscular fatigue<sup>1,5</sup>, determining the dynamic relation between rectified EMG and joint torque<sup>6,7</sup>, computing the conduction velocity of skeletal muscle in the presence of noise<sup>8-10</sup>, and examining the nonlinear relation between joint velocity and the stretch reflex<sup>11,12</sup>.

The variety of applications for the EMG has led to the development of numerous types of recording devices. The primary purpose of any EMG amplifier is to amplify the muscular potential, which typically has an RMS value of 100–1000  $\mu$ V, to a range that is both more easily measured, and less susceptible to the noise which can be a major factor when dealing with such small voltages. The main sources of noise present during EMG recordings include: power line interference, variations in skin impedance, offset

voltages due to the electrode/skin interface, and motion artefacts due to movements of the electrodes with respect to the muscle<sup>1</sup>. Many of these problems may be minimized by using differential amplifiers having a high input impedance, a high common-mode rejection ratio (CMRR), and a low zero-input noise level<sup>13-15</sup>. There are several methods for dealing with the DC offsets and the low-frequency artefacts. Many amplifiers incorporate a high-pass filter with a low cut-off frequency in order to eliminate these components. However, in applications where the gain and phase response are critical, the distortion associated with a high-pass filter which adequately removes all low-frequency artefact may not be tolerable. In these cases, amplifiers may employ a very low-frequency high-pass filter, or have a DC response and an input offset adjustment. Non-causal digital postprocessing may then be used to eliminate low-frequency noise.

The many uses for the EMG signal have led to the design and implementation of a wide variety of EMG amplifiers. It is therefore important to assess the relevant characteristics of an EMG amplifier quantitatively to understand its limitations, and to ensure that it is the proper choice for the situation at hand. The purpose of this work was to characterize the performance of four typical EMG amplifiers to demonstrate the diversity and specificity of some commonly used equipment.

## METHODS

### Amplifiers

Four amplifiers were tested:

1. The Liberty Mutual MYO 111 (Liberty Mutual, Hopkinton, Massachusetts) is a high input impedance amplifier built into a small package

Correspondence and reprint requests to: Robert E. Kearney

© 1993 Butterworth-Heinemann for BES  
0141-5425/93/05413-07

incorporating permanent surface electrodes of the type often used for prosthetic control. It is a high gain amplifier with a maximum gain of  $4600 \text{ V V}^{-1}$ , and a fixed bandpass response, centred at 150 Hz.

2. The Utah EMG preamplifier (ML22; Motion Control, a division of Iomed Inc., Salt Lake City, Utah) is also a high input impedance surface electrode, but was designed as a preamplifier with a gain of only  $315 \text{ V V}^{-1}$ , and hence many applications will require an additional gain stage. It has fixed lower and upper cut-off frequencies of 10 Hz and 30 kHz respectively.
3. The BMED1 amplifier was constructed in our laboratory approximately 10 years ago. The input stage comprises primarily a Burr-Brown 3620 instrumentation amplifier (Burr-Brown, Tucson, Arizona) located in a small box close to the subject. A separate remote amplifier provides additional gains and bandpass filtering. A representative gain of  $1000 \text{ V V}^{-1}$  and cut-off frequencies of 10 Hz and 1 kHz were used for these experiments.
4. The BMED2 amplifier was also constructed in our laboratory using more recent technology. It consists of an AD625 instrumentation amplifier (Analog Devices, Norwood, Massachusetts), a passive high-pass filter, and an AD210 isolation amplifier, enclosed in a small casing. The gain, which was switchable between 1000 and  $10\,000 \text{ V V}^{-1}$ , was set to  $1000 \text{ V V}^{-1}$ ; the high-pass cut-off point can be set by a single resistor and was fixed at 1 Hz.

All amplifiers, with the exception of the BMED1, were powered by an Anatek 6015 power supply. The MYO 111 and the Motion Control device were supplied with  $\pm 5 \text{ V}$ , and the BMED2 was supplied with  $+15 \text{ V}$ . The BMED1 unit contained its own power supply.

### Frequency response measurements

A Hewlett-Packard HP3562A dynamic signal analyser (Hewlett-Packard, Palo Alto, California) was used to make gain, phase and coherence measurements. The HP3562A has a 150 dB input range, with  $\pm 0.15 \text{ dB}$  accuracy over an 80 dB dynamic range. The real and the imaginary components of the frequency response were measured in both differential-mode and common-mode configurations. The resulting data were down-loaded to a Digital VAXstation 3100, where gain and phase characteristics were computed. The CMRR was computed by dividing the differential gain response by the common mode gain response.

Inputs to the BMED1 and the BMED2 were applied using standard electrode leads, soldered to a coaxial cable with a BNC connector. Inputs to the two active electrode devices were applied through securely fastened copper strips attached to a coaxial cable and BNC connector. For the differential measurements, the test signal was applied to one recording electrode; the second recording electrode and the reference electrode were tied to ground. For the common-mode measurements, the test signal was applied simultaneously to both recording inputs,

while the reference was tied to ground. The differential and common mode measurements were carried out with balanced inputs and with input load imbalances of 1, 10, and  $100 \text{ k}\Omega$ , generated by placing a precision resistor (Vishay S102K, with a 0.1% tolerance, and a  $+0.6 \text{ ppm } ^\circ\text{C}^{-1}$  temperature coefficient; Vishay Resistive Group, Malvern, Pennsylvania) in the signal path of the positive amplifier input.

The input test signal, generated by the HP3562A dynamic signal analyser, was a log resolution, swept sine signal which spanned the frequency range from 0.1 Hz to  $100 \text{ kHz}$  with a resolution of  $13.3 \text{ points decade}^{-1}$ . The dynamic signal analyser varied the input amplitude in an attempt to keep the output voltage constant over the entire frequency range, thereby increasing the measurement signal-to-noise ratio (S/N). The input amplitude never exceeded the input saturation level specified by the manufacturer of each device. Ten cycles were measured at each frequency, and used to compute the squared coherence between input and output. The squared coherence is a measure of the statistical variance between two or more averaged values, and can range between 0.0 and 1.0. Values lower than 1.0 typically indicate system nonlinearities or measurement noise but, in the swept sine mode of the HP3562A, harmonic distortion has little effect on the measured response, and hence the coherence estimate is predominantly an indication of the measurement noise.

### Noise measurements

Noise was measured using a Hewlett-Packard 3588A spectrum analyser, which has a measurement range extending to  $-132 \text{ dBm}$  and a maximum S/N range of  $-112 \text{ dB}$ . Measurements of the output noise for each amplifier were made over three frequency ranges: 5–110 Hz, 900 Hz– $10.1 \text{ kHz}$  and 10 Hz– $100 \text{ kHz}$ . These had resolution bandwidths of 1.1, 9.1 and 73 Hz respectively. For these measurements, all amplifiers except the BMED1 were powered by a low noise ( $<100 \mu\text{V RMS}$ ) Lambda LQD-421 (Lambda Electronics, Melville, NY) power supply. Noise measurements were made by grounding all amplifier inputs, and measuring the resulting output signal. The MYO 111, the motion control and the BMED2 devices were placed in a grounded Faraday box, in an attempt to reduce extraneous electromagnetic noise. The purpose of these precautions was to ensure that the noise measurements would properly characterize the amplifiers, as opposed to the environment within which they were tested. BMED1 was too large to be isolated in the Faraday box, and hence the results for this device are not as environmentally independent as those from the other amplifiers. Both the spectrum analyser and the power supplies were connected to the Faraday box with 200 mm coaxial cables.

## RESULTS

### Frequency response

The measured coherence for the differential response of each device with balanced input impedances was

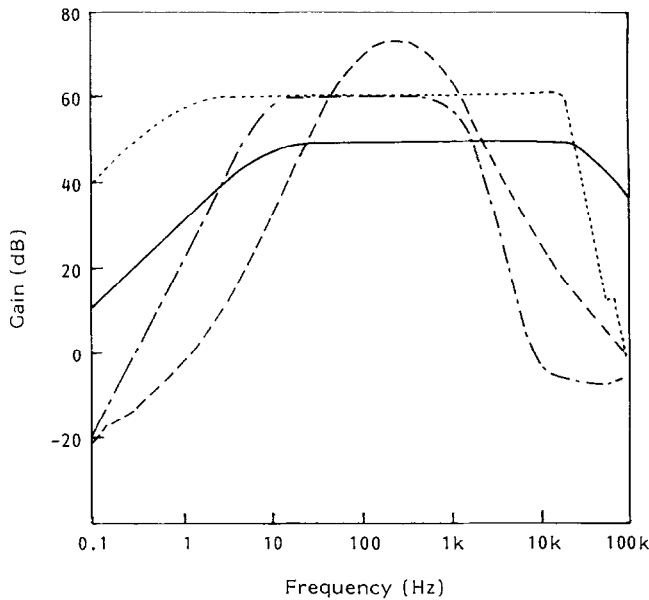


**Figure 1** Amplifier gain as a function of frequency. These were measured using an HP3562A, in the swept sinusoid mode. Input amplitude was adjusted in order to maximize the signal-to-noise ratio, and to avoid input saturation. --- MYO 111; — Motor Control; - · - · - BMED1, ..... BMED2

equal to 1.0 within the range of measured frequencies. The only exception was the BMED2, where the coherence was near zero for frequencies above the carrier frequency of the isolation amplifier. These high coherence values indicate that there was no significant measurement noise for the differential gain and phase response measurements.

The gain characteristics of the four devices are shown in *Figure 1*. It is evident that all but the MYO 111 have a constant gain response over some specific frequency range. Note that the BMED1 has externally adjustable cut-off frequencies; the upper and lower frequencies were merely chosen to illustrate typical experimental values. Applications which depend on the spectral characteristics of the EMG signal such as fatigue analysis would be best suited to wide bandwidth responses such as those of the Motion Control and BMED2 devices so that all portions of the frequency spectrum can be properly analysed. The expense of having a wideband constant gain amplifier is that motion artefact may not be properly filtered from the EMG signal. This is particularly likely for the BMED2 and Motion Control devices which have single-pole high-pass filters with respective cut-off frequencies of 1 Hz and 10 Hz. These amplifiers also have very high upper cut-off frequencies which may allow for extraneous high-frequency noise.

*Figure 2* shows the phase responses for each unit. Note that the phase responses for the BMED1 and BMED2 devices continue to extend below  $-180^\circ$  but these portions are omitted from *Figure 2* for sake of clarity. Because the phase of a linear system is usually related to the rate of change of the gain response<sup>16</sup>, it is not surprising that only the Motion Control and the BMED2 amplifiers have negligible phase shifts within the passband, due to their wideband gain responses. Because of their steep roll-offs outside the passband, and their narrowband gain responses, both the MYO 111 and the BMED1 devices have phase characteris-

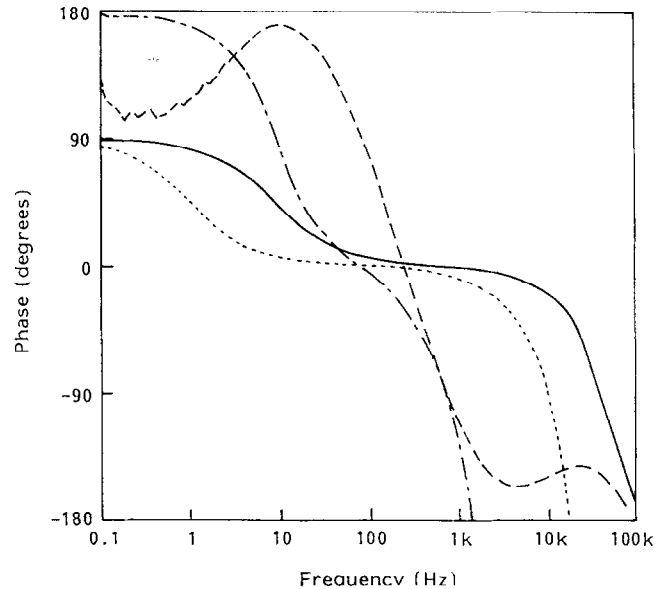


**Figure 2** Amplifier phase as a function of frequency. Key as for *Figure 1*

tics that vary almost constantly with frequency. In general, it is necessary to extend the cut-off frequencies approximately one decade above and below the frequency range where a linear phase shift is required. It is important to note that the phase characteristics of an amplifier with adjustable cut-off frequencies, such as the BMED1 device, can easily be modified, but fixed cut-off devices require digital postprocessing, or inverse filtering if the phase response needs to be altered.

### CMRR

*Figure 3* shows the common mode rejection ratio for the four amplifiers, evaluated as the ratio of the differential-mode gain and the common-mode gain. The coherence for the common mode gain measurements dropped below 1.0 at points where this gain was low, resulting in an output voltage too small to be accurately recorded by the HP3562A. For all devices

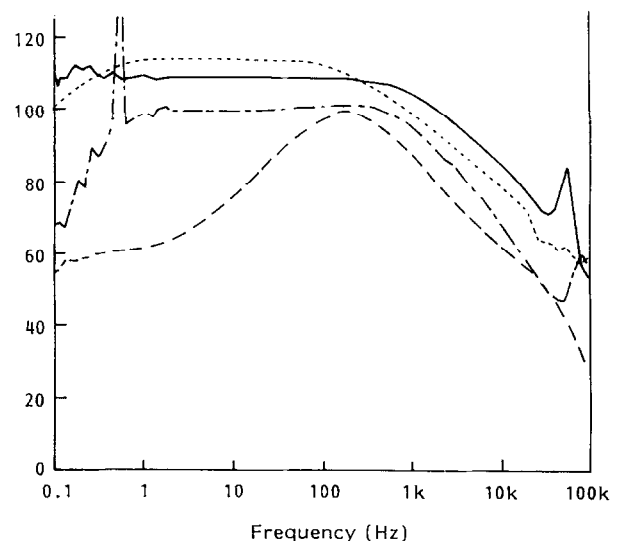


**Figure 3** CMRR for each device was computer by dividing the measured differential mode gain by the measured common mode gain. Key as for *Figure 1*

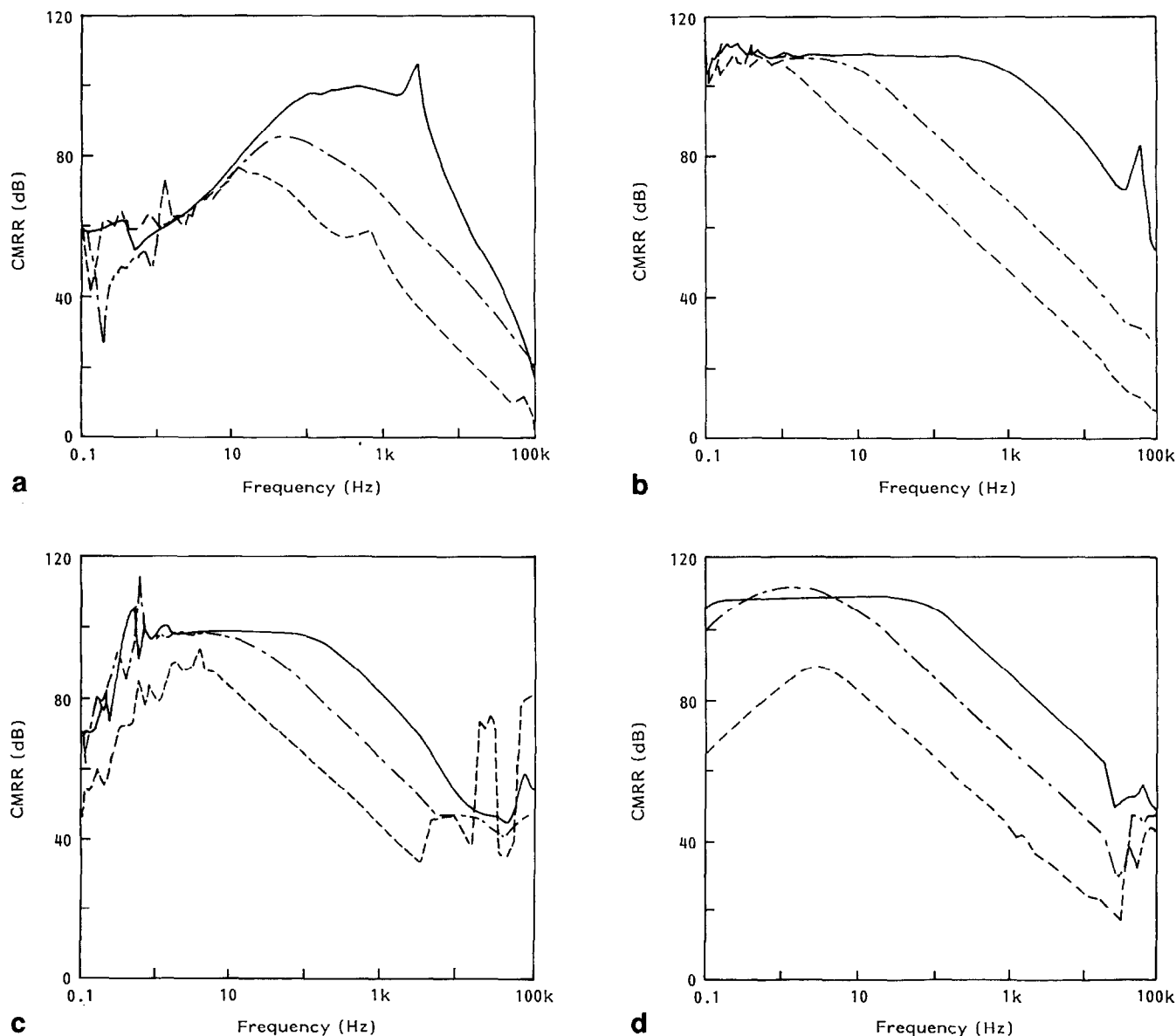


**Figure 4** CMRR measurements were repeated with input impedance mismatches of 1, 10 and 100 k $\Omega$ . Jagged portions of the curves indicate areas where the measurement noise was relatively high. Impedance imbalance: — 1 k $\Omega$ ; - - - 10 k $\Omega$ ; - · - 100 k $\Omega$ ; a, MYO 111; b, Motion Control; c, BMED1; d, BMED2

though, the coherence within the passband was close to 1.0, hence the CMRR measurements in this range are quite accurate. The low coherence ranges can be identified by the jagged peaks in the CMRR curves.

The CMRR with balanced input loads was found to be quite high within the passband of all devices, particularly the BMED2 and Motion Control amplifiers which had passband CMRRs greater than 105 dB. It is important though to notice the frequency dependence of the CMRR, which is often not addressed in the manufacturer's specifications.

The CMRR of each device was measured also with input impedance imbalances of 1, 10 and 100 k $\Omega$ . These imbalances were found to have little effect on the differential gain responses, but caused significant increases in the common mode responses of all devices. As a result, the CMRR was found to decrease drastically with increasing input load imbalance. These results are summarized in Figure 4. A 1 k $\Omega$  imbalance did not significantly alter the measured CMRR from the ideal case shown in Figure 3, but

larger mismatches noticeably degraded the performance of all devices. This degradation was most evident at higher frequencies where the CMRR dropped by as much as 50 dB.

#### Noise measurements

Figure 5 shows the output noise spectra, normalized to a 1 Hz measurement bandwidth, for each device. Note that the large spike in the noise spectrum for the BMED2 device is due to the 50 kHz oscillator. From these spectra, it can be seen that the amplifiers' noise characteristics are greatly effected by the frequency characteristics. For example, the MYO 111 and the BMED1 have relatively little noise power at higher frequencies, due to their low cut-off frequencies, but the noise power of the wideband amplifiers, particularly the BMED2 device, extends to higher frequencies.

Separate measurements were made at specific frequencies which better represent the common range

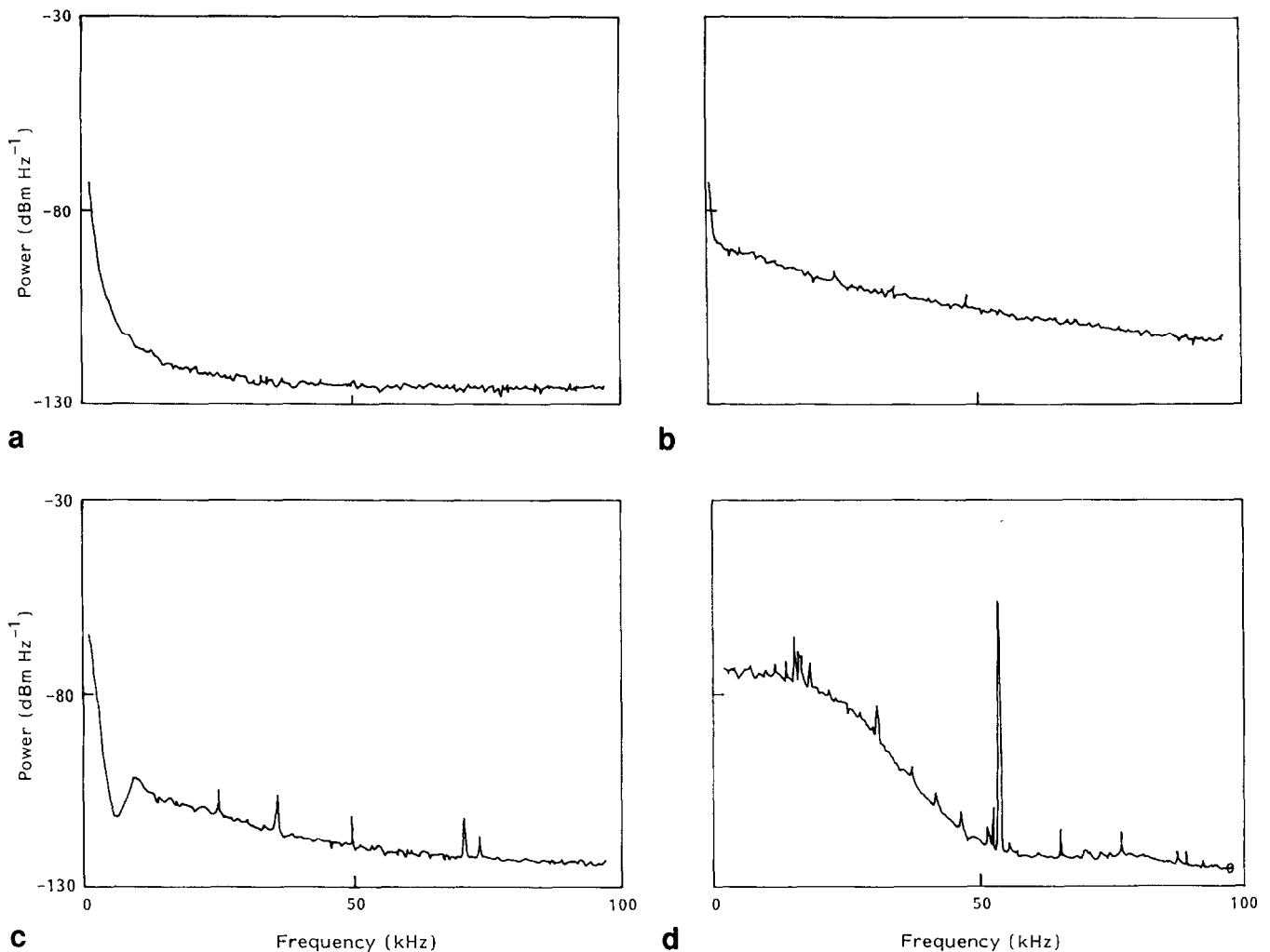


**Figure 5** Output noise spectra, normalized to a 1 Hz measurement bandwidth; the actual measurement bandwidth was 73 Hz: **a**, MYO 111; **b**, Motion Control; **c**, BMED1; **d**, BMED2

of EMG measurements. In order to compensate for the different amplification of each amplifier, these measurements were normalized with respect to the passband gain of each device. The output noise below 1 kHz was also estimated by integrating the noise spectra below 1 kHz and normalizing the results to an amplifier passband gain of  $1000 \text{ V V}^{-1}$ . The noise analysis results are summarized in *Table 1*.

The MYO 111 was found to have significantly better noise characteristics than the other tested amplifiers but in all cases the noise measured below

1 kHz was minimal. In light of this, it is likely that, during an experimental situation, environmental noise and inadequately rejected common-mode signal components will account for most of the measurement noise.

## DISCUSSION

Ideally, an EMG amplifier would amplify the signal with no added distortion, but because of practical considerations, no amplifier is ideal for all possible experimental set-ups. Depending on the intended use of the device, design trade-offs are generally made during amplifier construction. Thus it is not surprising that the four tested amplifiers have a broad range of characteristics.

### Gain and phase characteristics

An ideal amplifier should have flat gain and phase responses over the entire range of input frequencies, which for an EMG signal is typically from about 25 Hz to several kilohertz<sup>17</sup>. The flat response of an amplifier/electrode combination ensures that any frequency domain comparisons are not tainted by the measuring device. *Figures 1* and *2* show that only the Motion Control and the BMED2 devices had a flat

**Table 1** Noise levels

Amplifier	Input noise ( $\text{nV}/\sqrt{\text{Hz}}$ )				Normalized RMS output noise (mV) below	
	10 kHz	60 Hz	100 Hz	1 kHz	10 kHz	1 kHz
MYO 111	1.5	7.4	9.6	5.2	0.1	0.2
Motion Control	42	690	55	31	15	1.6
BMED1	280	1250	111	73	1.3	3.9
BMED2	100	500	160	78	32	3.2

The input noise levels were estimated by dividing the normalized output noise with the passband gain. The measurement bandwidths were 1.1 Hz for the 10 Hz, 60 Hz and 100 Hz measurements, and 9.1 Hz for the 1 kHz and 10 kHz measurements. The output noise levels were estimated by normalizing the measured spectra to an overall passband gain of  $1000 \text{ V V}^{-1}$ , and integrating below 1 kHz

gain response and negligible phase shift for a significant portion of the passband. This was due to the low cut-off frequency, and first-order roll-off of the high-pass filters, as well as the high upper cut-off frequencies. A flat response becomes important when the EMG signal is being used for system identification purposes since the relative timing or phase shift between all signals is fundamental to obtaining meaningful results. If the amplifier has a linear response, it is theoretically possible to compensate for a non-ideal spectral response by deconvolving the amplifier response from the measured signal. In practice though, if the actual response has significantly less bandwidth than the desired response, deconvolution will result in noise amplification and, hence, cannot practically be used to compensate for large deviations from the desired behaviour.

The cost of having a flat low-frequency response will be an increase in motion artefact. These artefacts can be removed by digital postprocessing without affecting the phase characteristics of the signal; however, to avoid saturation due to this additional artefact, it may be necessary to decrease the amplifier gain, possibly reducing the measurement signal-to-noise ratio. For applications where postprocessing is not feasible, such as in prosthetic control or biofeedback, built in high-pass filters for removing low-frequency artefacts are essential. The frequency response of the MYO 111 is well suited to this type of situation.

Upper cut-off frequencies higher than necessary will increase high-frequency noise, but if the signal is to be recorded by an A/D converter, this high-frequency noise will be eliminated by proper anti-aliasing filters. Otherwise, it is useful to have an amplifier with an adjustable upper cut-off frequency tailored for each specific use to provide the desired gain and phase characteristics, as well as high-frequency noise reduction.

### CMRR and input impedance

Ambient electromagnetic signals, particularly 60 Hz power noise and its harmonics, are often much larger than the desired neuromuscular signal of interest<sup>18</sup>. The use of differential amplifiers to reduce this noise is well documented<sup>19</sup>. The inputs to a differential EMG amplifier typically can be separated into common-mode and differential-mode components; only the latter is generally of interest. The effectiveness of the differential amplifier in removing common-mode components of a signal is measured by its CMRR, which is the ratio of the differential-mode gain to the common-mode gain. It is critical to have a high common-mode rejection within the passband. Ideally, the CMRR of an EMG amplifier should be infinite, but nonlinearities and problems in the matching of component values typically limit the CMRR to between 60 dB and 130 dB. Although CMRR is often specified by a single value, it is evident from *Figure 3* that the CMRR is extremely frequency dependent. Care must be taken to ensure that the CMRR is adequate over the entire frequency range of interest. Under ideal considerations (i.e. no input impedance mismatches), the CMRR was found

to be high within the passband of all amplifiers, particularly the Motion Control and the BMED2 devices.

Under practical situations, the effective CMRR of an amplifier can be drastically lowered by impedance mismatches between the two differential inputs, particularly in the presence of low common-mode input impedances<sup>13,18</sup>. *Figure 4* shows that the CMRR could be reduced by as much as 50 dB with a 100 k $\Omega$  input impedance mismatch. Olson<sup>20</sup> reported mismatches as high as 50 k $\Omega$  for unprepared skin; mild abrasions were shown to decrease this impedance by approximately 26 dB. Our results suggest that even though the differential gain responses of these high differential input impedance devices were not affected by large impedance mismatches, the noise rejection capabilities of all the tested amplifiers could be greatly improved with pre-experimental skin preparation.

The effect of the common-mode signal will also be reduced if the common-mode signal itself is reduced. This provision has the added benefit of helping to avoid input saturation, which can be potentially destructive to the amplifier. Typically, the reduction of the common-mode voltage is carried out by utilizing a third reference electrode, in order to create a virtual ground, or by using a boot-strapped two-electrode configuration, including a self-biasing path<sup>18</sup>. All of the amplifiers which were analysed used a third reference electrode, with the exception of the MYO 111, which is a two-electrode device.

### Noise

The input noise of an amplifier limits the resolution. Below the input noise level, it becomes difficult to distinguish stochastic EMG signals from noise. *Figure 5* shows that the wideband noise levels were greatly affected by the gain characteristics of each device. Both the MYO 111 and the BMED1 had very little high-frequency noise due to their low upper cut-off frequency. Most high-frequency noise, such as the 50 kHz peak in the BMED2 noise spectrum which was caused by the AD210's oscillation frequency, can be eliminated by the anti-aliasing filters necessary for proper A/D conversion, and is therefore insignificant for applications where the EMG signal is recorded. In feedback applications, where the signal may not be processed, excess high-frequency noise can be detrimental. *Table 1* indicates that with the exception of the 60 Hz rejection by the Motion Control device, the compact active electrode modules, especially the MYO 111, had the best noise characteristics in the commonly used frequency ranges. It is important to note that these measurements were taken under near ideal conditions; in a true experimental situation, where a shielded environment may not be feasible, the CMRR of each device, as well as other issues such as shielded cables and short connections, will play an important role in determining the noise characteristics of each device.

The other major difference between the amplifiers is that the MYO 111 and the Motion Control device have both the amplifier and the electrodes incorporated into the same compact package. This elimin-

ates electrode leads and will reduce noise during experimental situations as well as allowing for an uncluttered, convenient experimental set-up. Without modification however, such devices do not allow for flexibility in electrode choice. During experiments of long duration or those which require considerable movement, these electrodes may become impractical due to the external fixations needed for secure attachment. In such cases, self-adhesive electrodes may prove to be more convenient. The BMED2 does not incorporate electrodes directly into the differential input stage, but it is still small enough to be placed close to the muscle, thereby reducing the electrode lead length. The BMED1 represents an older device which is not as portable as any of the others, although conveniently has adjustments for selectable gains, cut-off frequencies, and an input offset which allows versatility over a wide range of experimental situations.

## CONCLUSIONS

These results describe the differing characteristics of four common EMG amplifiers designed for different applications. The MYO 111 is at one extreme: it is an extremely convenient, low-noise, small device, but does not have flat gain and phase responses within the passband; at the other is the BMED2, which has very accurate gain and phase responses, and a high CMRR, yet is not as convenient as the fully packaged devices. Amplifiers such as the MYO 111 would be most convenient in areas such as prosthetic control or biofeedback, where estimates of average muscular activity are required. Applications where more accurate measures of the EMG's amplitude and phase properties are required, such as many areas of system identification, would benefit most from flatter gain and phase responses such as those of the Motion Control and the BMED2 amplifiers. It should be noted that it is possible to order modified versions of the MYO 111 which have gain characteristics different from the standard model that we tested.

It was also found that the CMRR of all devices was drastically reduced in the presence of large input impedance mismatches. This was found to result from an increasing common-mode gain, and suggests that the noise rejection capabilities of all amplifiers will be improved with the aid of pre-experimental skin preparation, regardless of the amplifier's differential input impedance.

## ACKNOWLEDGEMENTS

This work was supported by the Medical Research Council of Canada and the Natural Sciences and Engineering Research Council of Canada. We would also like to thank Dr Stephen Jacobsen of the

University of Utah and his colleagues from Iomed, Inc., for the loan of the Motion Control amplifiers.

## REFERENCES

1. Basmajian JV, and De Luca CJ. *Muscles Alive*. Baltimore: Williams & Wilkins 1985.
2. Jones LA, Hunter IW. The relation of muscle force and EMG to perceived force in human finger flexors. *Eur J Appl Physiol* 1982; **50**: 125-31.
3. Milner-Brown HS, Stein RB. The relation between surface electromyogram and muscular force. *J Physiol* 1975; **246**: 549-69.
4. Stephens JA, Taylor A. The relation between integrated electrical activity and force in normal and fatiguing human voluntary contraction. In: Desmedt JE, ed. *New Development in Electromyography and Clinical Neurophysiology*. Basel: Karger, 1973, 623-7.
5. Kirsch RF, Rymer WZ. Neural compensation for muscular fatigue: evidence for significant force regulation in man. *J Neurophysiol* 1987; **57**: 1893-1920.
6. Genadry WF, Kearney RE, Hunter IW. Dynamic relationship between EMG and torque at the human ankle: variation with contraction level and modulation. *Med Biol Eng Comput* 1988; **26**: 489-96.
7. Lago PJ, Jones NB. Parameter estimation of system dynamics with modulation-type noise - application to the modelling of the dynamic relationship between the EMG and force transients in muscle. *IEEE Proc* 1984; **131D**: 221-8.
8. Rababy N, Kearney RE, Hunter IW. Method for EMG conduction velocity estimation which accounts for input and output noise. *Med Biol Eng Comput* 1989; **27**: 125-9.
9. Arendt-Nielsen L, Zwarts M. Measurement of muscle fiber conduction velocity in humans: techniques and applications. *J Clin Neurophysiol* 1989; **6**: 173-90.
10. Hunter IW, Kerney RE, Jones LA. Estimation of the conduction velocity of muscle action potentials using phase and impulse response function techniques. *Med Biol Eng Comput* 1987; **25**: 121-6.
11. Kearney RE, Hunter IW. Nonlinear identification of stretch reflex dynamics. *Ann Biomed Eng* 1988; **16**: 79-94.
12. Soechting JF, Dufresne JR. An evaluation of nonlinearities in the motor output response to applied torque perturbations in man. *Biol Cybern* 1980; **36**: 63-71.
13. Scott RN, Lovely DF. Amplifier input impedances for myoelectric control. *Med Biol Eng Comput* 1986; **24**: 527-30.
14. Metting van Rijn AC, Peper A, Grimbergen CA. High-quality recording of bioelectric events. *Med Biol Eng Comput* 1990; **28**: 389-97.
15. Pallás-Areny, Webster JG. Composite instrumentation amplifier for biopotentials. *Ann Biomed Eng* 1990; **18**: 251-62.
16. Bode HW. *Network Analysis and Feedback Amplifier Design*. New York: Van Nostrand, 1945.
17. Neuman MR, Biopotential amplifiers. In: Webster JG, ed. *Medical Instrumentation - Application and Design*. Boston: Houghton Mifflin, 1978.
18. Winter BB, Webster JG. Reduction of interference due to common mode voltage in biopotential amplifiers. *IEEE Trans Biomed Eng* 1983; **30**: 58-62.
19. Horowitz P, Hill W. *The Art of Electronics*. New York: Cambridge University Press, 1989, Chs 2, 7.
20. Olson WH, Schmincke DR, Henley BL. Time and frequency dependence of disposable ECG electrode-skin impedance. *Medical Instrumentation* 1979 **13**: 269-72.